Brazilian Journal of Physics (2019) 49:151–160
https://doi.org/10.1007/s13538-018-00628-3

SOCIEDADE BRASILEIRA DE FÍSICA

ATOMIC PHYSICS

Dielectric, Photophysical, Solvatochromic, and DFT Studies on Laser Dye Coumarin 334

C. V. Maridevarmath[1] · Lohit Naik[2] · G. H. Malimath[2]

Received: 18 September 2018 / Published online: 7 January 2019

Abstract

The absorption and fluorescence spectra of laser dye, 10-acetyl-2,3,6,7-tetrahydro-1H,5H,11H-pyrano[2,3-f]pyrido[3,2,1-ij]quinolin-11-one [C-334], are recorded. The ground-state dipole moments (μ_g) were determined from density functional theory (DFT) computations, Guggenheim's, and solvatochromic methods. The excited-state dipole moments (μ_e) were determined from Lippert's, Bakhshiev's, Kawski-Chamma-Viallet's, and McRae's equations. The μ_e values are found to be higher than μ_g values and this suggest that the probe molecule is more polar in the excited state. The absorption maxima and emission maxima of C-334 undergo bathochromic shift as the polarity of the solvent increases and indicates that the transitions involved are $\pi \rightarrow \pi^*$. The change in dipole moment ($\Delta\mu$) and the angle between μ_e and μ_g is calculated. The absorption and fluorescence emission of the probe C-334 were investigated theoretically with the help of Gaussian 09W for all the studied solvents by using time-dependent (TD)-DFT combined with conductor-like polarizable continuum model (CPCM) solvation model and were compared with the experimental results. Further, the ground- and excited-state dipole moments were also estimated for all the studied solvents by using CPCM solvation model and are compared with the experimental results. The HOMO-LUMO energy gaps computed using DFT and from absorption threshold wavelengths are found to be in order with each other. The chemical hardness (η) of the probe molecule is estimated and the results suggest the soft nature of the molecule. Further, the reactive centers like electrophilic site and nucleophilic site were identified with the help of molecular electrostatic potential (MESP) 3D plots using DFT computational analysis.

Keywords Coumarin 334 · Guggenheim's method · Solvatochromic · DFT · HOMO-LUMO

1 Introduction

Coumarin and their derivatives represent a class of well-known laser dyes in the blue-green spectral region, characterized by high-emission quantum yields and find many practical applications in the various fields of science and technology. Since they exhibit fluorescence in the UV-Vis region, they are used as colorants, dye lasers, and non-linear optical fluorophores [1–3]. They are used as photo initiators, emission layers in organic light-emitting diodes, probes in the biological study, photodimerization in polar, non-polar solvents, etc. [4–6]. They also find applications as fluorescent indicators [7], optical brighteners [8], sunscreens [9], anti-coagulants, biological and chemical sensors [10, 11], in enzymology [12], blood thinners [13], anti-inflammatory [14], anti-tubercular [15], anti-HIV [16], and anti-cancer [17] agents.

Recently, there are reports on using C-334 as an atypical antioxidant [18], electroosmotic flow marker for characterization of carbon quantum dots [19], EOF marker for investigating doxorubicin encapsulation [20], and off–on catalytic chemodosimeter for Cu^{2+} ions [21], to form single, binary, ternary dye-doped PMMA thin films [22].

The solvatochromic investigations aimed at determination of dipole moments in the ground and excited state are important, as they furnish information about the changes in electronic distribution and symmetry of the molecule in the excited state. The μ_e value of the molecule is found to be helpful in designing the non-linear optical materials. Further, it also helps in determining the electrophilic and nucleophilic sites, which are useful in photochemical reactions, etc. It is observed that the electronic spectra of molecules are influenced by their

✉ G. H. Malimath
gurukcd@gmail.com

[1] Department of Physics, Government First Grade College, Hubballi, Karnataka 580032, India

[2] UG and PG Department of Physics, Karnataka Science College, Dharwad, Karnataka 580001, India

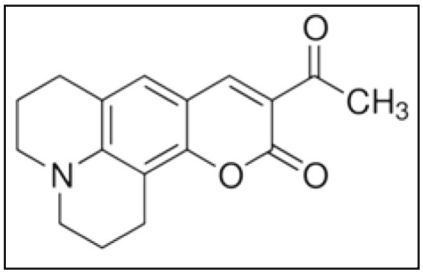

Fig. 1 Molecular structure of C-334

immediate environment [2–6, 23–30]. For the determination of dipole moments, there are numbers of methods like electric dichroism [31], electric polarization of fluorescence [32], microwave conductivity [33], and Stark splitting [34] that are available. However, their use is limited as they are considered to be equipment intensive and applicable to relatively simple molecules. On the other hand, Guggenheim's [35] and solvatochromic methods offer simple techniques to determine the dipole moments of the probe molecules.

Earlier, our research group has reported on resonance energy transfer studies on derivatives of thiophene substituted 1,3,4-oxadiazoles and C-334 laser dye in different media [36]. In the present work, the ground-state dipole moment (μ_g) and excited-state dipole moment (μ_e) of C-334 are determined from dielectric, solvatochromic, and DFT studies, the HOMO-LUMO energy gap, chemical hardness, and molecular electrostatic potential (MESP) plots have been studied, and the results obtained are presented and discussed.

2 Theory

2.1 Ground-State Dipole Moment by Guggenheim's Method

According to Guggenheim's [35] method, the ground-state dipole moment (μ_g) is given by

$$\mu_g^2 = \left[\frac{27kT}{4\pi N(\varepsilon_1+2)\left(n_1^2+2\right)}\right]\Delta \tag{1}$$

$$\text{where}\quad \Delta = \left[\left(\frac{\varepsilon_{12}-\varepsilon_1}{C}\right)c_{\to 0} - \left(\frac{n_{12}^2-n_1^2}{C}\right)c_{\to 0}\right] \tag{2}$$

The symbols k, T, N, ε, C, and n represent Boltzmann's constant, absolute temperature, Avogadro's number, dielectric constant, concentration, and refractive index respectively. The suffixes 12, 1, and 2 correspond to the solution, solvent, and solute respectively. The symbol "Δ" represents the difference in the extrapolated intercepts from the plots $(\varepsilon_{12}-\varepsilon_1)/C$ vs. C and $({n_{12}}^2-{n_1}^2)/C$ vs. C corresponding to infinite dilution ($C \to 0$). The value of ε_{12} is calculated by using Eq. (3).

$$\varepsilon_{12} = \frac{C_{12}-C_1}{C_a-C_1} \tag{3}$$

where c_{12} is the capacitance of cylindrical cell with solution and c_a is the capacitance of cylindrical cell without solution respectively. c_1 represents connecting leads' capacitance. The suffixes 12, 1, and 2 refer to the solution, solvent, and solute respectively.

2.2 Ground- and Excited-State Dipole Moments by Solvatochromic Method

The μ_g and μ_e values are calculated using the solvatochromic equations.

The expression for Stoke's shift according to Lippert's [37] is given as

$$\overline{\upsilon}_a - \overline{\upsilon}_f = SF(\varepsilon, n) + const \tag{4}$$

where $F(\varepsilon, n)$ is Lippert's polarity function and is given as

$$F(\varepsilon, n) = \left[\frac{\varepsilon-1}{2\varepsilon+1} - \frac{n^2-1}{2n^2+1}\right] \tag{5}$$

The expression for Stoke's shift according to Bakhshiev's [38] is

Table 1 Dielectric constants and refractive indices of C-334 dye in benzene (dielectric constant and refractive index of benzene are $\varepsilon_1 = 2.3304$ and $n_1 = 1.4990$)

Wt. fraction (C)	Dielectric const of solution (ε_{12})	$(\varepsilon_{12}-\varepsilon_1)/C$	Refractive index of solution (n_{12})	${n_{12}}^2$	$({n_{12}}^2-{n_1}^2)/C$	Δ′	Δ″	Δ = Δ′ − Δ″
0.00819	2.630	36.630	1.5015	2.254	0.915	149	1.770	147.230
0.00600	2.615	47.583	1.5010	2.253	1.000			
0.00400	2.488	39.450	1.5005	2.251	1.124			
0.00296	2.437	36.013	1.5000	2.250	1.013			
0.00098	2.417	88.367	1.4995	2.248	1.529			

Table 2 Solvatochromic data of C-334

Solvent	λ_a (nm)	λ_f (nm)	$\bar{\upsilon}_a$ (cm^{-1})	$\bar{\upsilon}_f$ (cm^{-1})	$\bar{\upsilon}_a - \bar{\upsilon}_f$ (cm^{-1})	$(\bar{\upsilon}_a + \bar{\upsilon}_f)/2$ (cm^{-1})
Benzene	444	479	22,522.523	20,876.827	1645.696	21,699.675
Tetrahydrofuran	444	484	22,522.523	20,661.157	1861.365	21,591.840
Propane-2-ol	453	496	22,075.055	20,161.290	1913.765	21,118.173
Acetone	449	496	22,271.715	20,161.290	2110.425	21,216.503
Ethanol	451	501	22,172.949	19,960.080	2212.869	21,066.514
Methanol	453	505	22,075.055	19,801.980	2273.075	20,938.518
Acetonitrile	447	498	22,371.365	20,080.321	2291.043	21,225.843

$$\overline{\upsilon}_a - \overline{\upsilon}_f = S_1 F_1(\varepsilon, n) + const \tag{6}$$

where $F_1(\varepsilon, n)$ is Bakhshiev's polarity function and is given as

$$F_1(\varepsilon, n) = \frac{2n^2+1}{n^2+2}\left[\frac{\varepsilon-1}{\varepsilon+2} - \frac{n^2-1}{n^2+2}\right] \tag{7}$$

According to Kawski-Chamma-Viallet's [39] equation,

$$\frac{1}{2}\left(\overline{\upsilon}_a + \overline{\upsilon}_f\right) = S_2 F_2(\varepsilon, n) + const \tag{8}$$

where $F_2(\varepsilon, n)$ is Kawski-Chamma-Viallet's polarity function and is given as

$$F_2(\varepsilon, n) = \frac{2n^2+1}{2(n^2+2)}\left[\frac{\varepsilon-1}{\varepsilon+2} - \frac{n^2-1}{n^2+2}\right] + \frac{3}{2}\left[\frac{n^4-1}{(n^2+2)^2}\right] \tag{9}$$

According to McRae's [40] equation,

$$\overline{\upsilon}_a = -S_3 F_3(\varepsilon) + const \tag{10}$$

where $F_3(\varepsilon)$ is McRae's polarity function and is given as

$$F_3(\varepsilon) = \left[\frac{2(\varepsilon-1)}{\varepsilon+2}\right] \tag{11}$$

From the above Eqs. (4), (6), (8), and (10), it follows that $(\bar{\upsilon}_a - \bar{\upsilon}_f)$ vs. $F(\varepsilon,n)$, $(\bar{\upsilon}_a - \bar{\upsilon}_f)$ vs. $F_1(\varepsilon,n)$, $1/2(\bar{\upsilon}_a + \bar{\upsilon}_f)$ vs. $F_2(\varepsilon,n)$, and $\bar{\upsilon}_a$ vs. $F_3(\varepsilon)$ should give linear graphs with slopes S, S_1, S_2, and S_3 and are given as

$$S = \frac{2\left(\mu_e - \mu_g\right)^2}{hca_0^3} \tag{12}$$

$$S_1 = \frac{2\left(\mu_e - \mu_g\right)^2}{hca_0^3} \tag{13}$$

$$S_2 = \frac{2\left(\mu_e^2 - \mu_g^2\right)}{hca_0^3} \tag{14}$$

$$S_3 = \frac{\mu_g\left(\mu_e - \mu_g\right)}{hca_0^3} \tag{15}$$

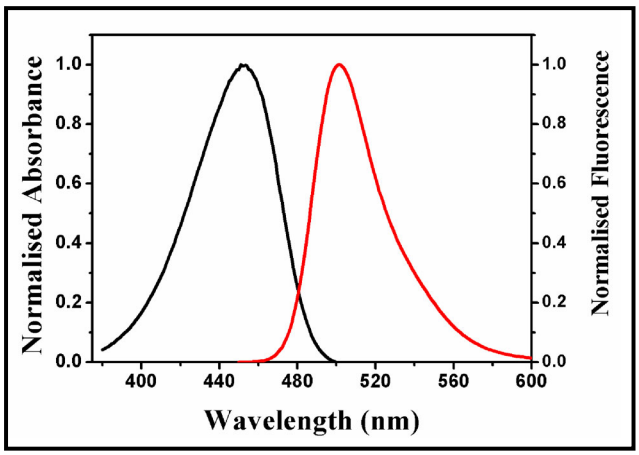

Fig. 2 Absorption and fluorescence spectra of C-334 in ethanol

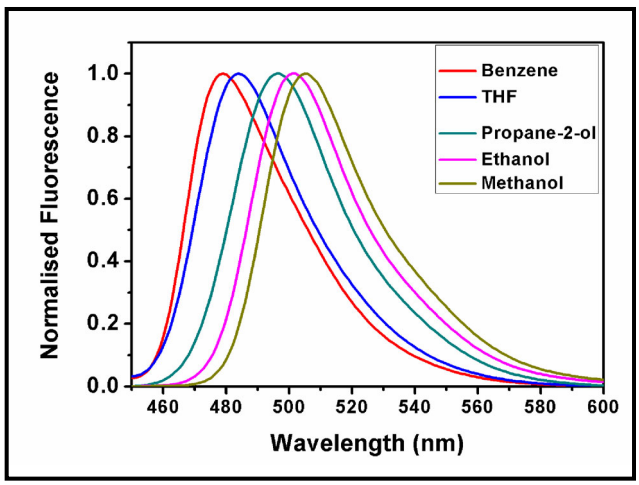

Fig. 3 Fluorescence spectra of C-334 in different solvents

Table 3 Some physical constants along with the calculated values of various polarity functions

Solvent	ε	n	E_T^N	$F(\varepsilon,n)$	$F_1(\varepsilon,n)$	$F_2(\varepsilon,n)$	$F_3(\varepsilon)$
Benzene	2.280	1.501	0.111	1.089	0.322	− 0.209	0.286
Tetrahydrofuran	7.580	1.405	0.207	0.987	0.312	− 0.202	0.237
Propane-2-ol	20.180	1.377	0.546	0.540	0.289	− 0.113	0.223
Acetone	21.010	1.359	0.355	0.794	0.305	− 0.174	0.213
Ethanol	24.300	1.361	0.654	0.405	0.262	− 0.076	0.214
Methanol	33.700	1.329	0.762	0.284	0.218	− 0.039	0.197
Acetonitrile	36.640	1.344	0.460	0.647	0.295	− 0.145	0.205

where μ_e and μ_g have their usual meaning and h and c correspond to Planck's constant and velocity of light respectively. The radius of the solute molecule "a_0" is of the order of 3.939 Å and its value is determined by using Edward's [41] atomic increment method.

Assuming that μ_e and μ_g are parallel to each other and upon electronic transition, the symmetry of the probe molecule remains same, based on Eqs. (13) and (14), one obtains

$$\mu_g = \frac{S_2 - S_1}{2}\left[\frac{hca_0^3}{2S_1}\right]^{1/2} \tag{16}$$

$$\mu_e = \frac{S_1 + S_2}{2}\left[\frac{hca_0^3}{2S_1}\right]^{1/2} \tag{17}$$

$$\mu_e = \frac{S_1 + S_2}{S_2 - S_1}\mu_g; (S_2 > S_1) \tag{18}$$

If the angles between μ_e and μ_g are not parallel, then the angle θ between the two dipole moments can be obtained from Eqs. (16) and (17) and is given by Eq. (19).

$$\cos\theta = \frac{1}{2\mu_g\mu_e}\left[\left(\mu_g^2 + \mu_e^2\right) - \frac{S_2}{S_3}\left(\mu_e^2 - \mu_g^2\right)\right] \tag{19}$$

2.3 Change in Dipole Moment ($\Delta\mu$) and Excited-State Dipole Moment (μ_e) by Solvent Polarity parameter $\left(E_T^N\right)$

This method is based on solvent polarity parameter $\left(E_T^N\right)$ to estimate change in dipole moment proposed by Reichardt [42] and developed by Ravi et al. [43]. The expression for spectral band shift with $\left(E_T^N\right)$ is given by Eq. (20).

$$\overline{\upsilon}_a - \overline{\upsilon}_f = 11307.6\left[\left(\frac{\Delta\mu}{\Delta\mu_B}\right)^2\left(\frac{a_B}{a_0}\right)^3\right]E_T^N + const \tag{20}$$

where $\Delta\mu_B = 9\ D$ represents the change in dipole moment and $a_B = 6.2$ Å denotes Onsager cavity radius of reference betaine dye molecule and $\Delta\mu$ and "a" are the respective quantities of the probe molecule. The $\Delta\mu$ can be determined from Eq. (21).

$$\Delta\mu = \sqrt{\frac{m \times 81}{\left(\frac{6.2}{a_o}\right)^3 11307.6}} \tag{21}$$

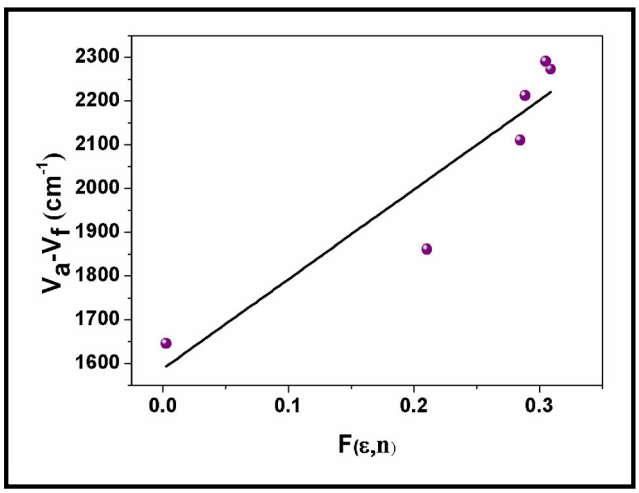

Fig. 4 Plot of Stoke's shift vs. $F(\varepsilon,n)$ using Lippert's equation

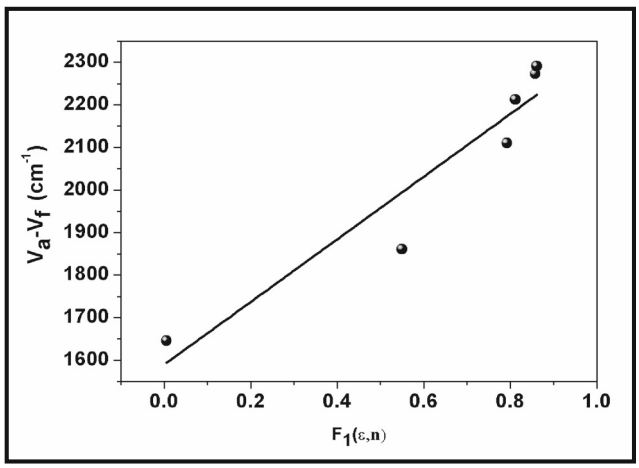

Fig. 5 Plot of Stoke's shift vs. $F_1(\varepsilon,n)$ using Bakhshiev's equation

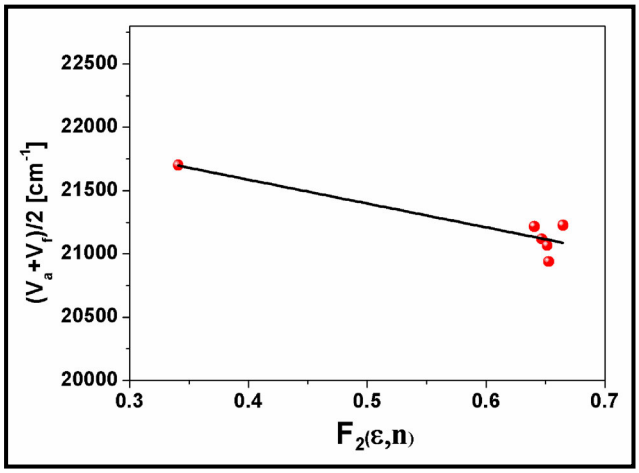

Fig. 6 Plot of arithmetic mean of Stoke's shift vs. $F_2(\varepsilon,n)$ using Kawski-Chamma-Viallet's equation

where m is the slope from the linear plot of Stoke's shift vs. $\left(E_T^N\right)$.

Knowing the value of $\Delta\mu$ and μ_g (from Eq. (1)), the excited-state dipole moment (μ_e) can be determined from Eq. (22).

$$\mu_e = \Delta\mu + \mu_g \tag{22}$$

3 Experimental

3.1 Materials Used

The laser dye C-334 is procured from Sigma-Aldrich, USA, and is used without any further purification. The molecular structure of C-334 is given in Fig. 1. All the solvents benzene, tetrahydrofuran (THF), propane-2-ol, acetone, ethanol, methanol, and acetonitrile are procured from S.D. Fine Chem. Pvt. Ltd., India, and are of spectroscopic grade. The various solutions were prepared at a fixed solute concentration of the order of 10^{-5} M in order to minimize self-absorption and aggregation formation.

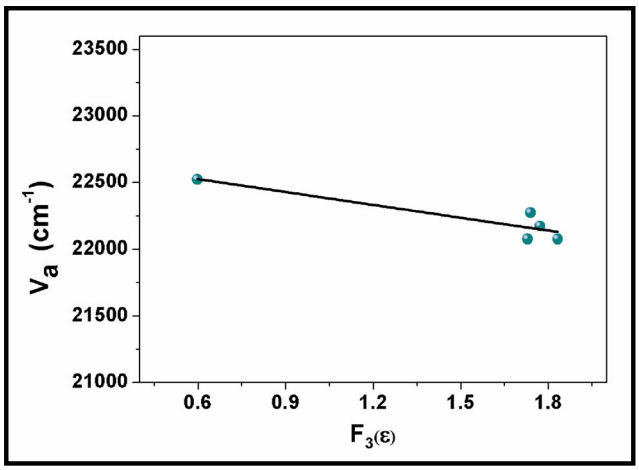

Fig. 7 Plot of $\bar{\upsilon}_a$ vs. $F_3(\varepsilon)$ using McRae's equation

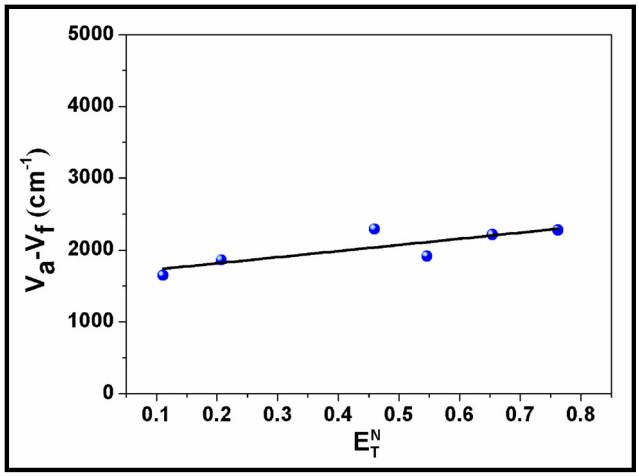

Fig. 8 Plot of Stoke's shift vs. $\left(E_T^N\right)$

3.2 Methods

The ε values of the various solutions are determined using a calibrated brass cell by using LCR Data Bridge (Aplab MT-4080D) at 10 kHz frequency. The refractive indices of various dilute solutions are determined by using Abbe's refractometer. Absorption and emission spectra were recorded using Specord 200 plus spectrophotometer and Hitachi F-7000 spectrofluorometer respectively. Theoretical computations were performed using DFT with basis sets B3LYP/6-31G (d).

4 Results and Discussions

4.1 Determination of Ground- and Excited-State Dipole Moments from Different Methods

The ε values of the different solutions (ε_{12}) are calculated by using Eq. (3). The refractive indices for various concentrations (n_{12}) are measured using Abbe's refractometer and the results are given in Table 1.

Table 4 Slopes, intercepts, and correlation coefficients

Correlations	Slope (cm^{-1})	Intercepts (cm^{-1})	Correlation coefficient
Lippert's correlation	2046.370	1588.162	0.846
Bakhshiev's correlation	736.617	1589.584	0.879
Kawski-Chamma-Viallet's correlation	1880.671	22,338.521	0.829
McRae's correlation	322.477	22,718.182	0.834

Table 5 Ground-state dipole moments by DFT, Guggenheim's, and solvatochromic methods

	Ground-state dipole moment (μ_g) (D) from	
DFT computations	Guggenheim's method Eq. (1)	Solvatochromic method Eq. (16)
8.501	1.086	1.642

Then from the knowledge of experimentally measured values of dielectric constant and refractive index of benzene and C-334 solutions, using Eq. (1), the μ_g value is calculated according to Guggenheim's method and the result is presented in Table 5.

The absorption and emission maxima, Stoke's shift, and arithmetic mean of Stoke's shift values in different solvents are presented in Table 2.

The absorption spectra of C-334 in ethanol and fluorescence spectra of C-334 in different solvents are shown in Figs. 2 and 3 respectively. From Fig. 3, it is observed that the emission maxima undergo a bathochromic shift as the polarity of solvent increases and this indicates the spectral transition to be $\pi \rightarrow \pi^*$.

From Table 2, it is observed that, for different solvents of increasing polarity, the absorption maxima show shifts from 22,522 to 22,075 cm^{-1} and emission maxima show shift from 20,876 to 19,801 cm^{-1}. Further, it is observed that the spectral shift in the emission spectra is large compared to the absorption spectra. This suggests that in the ground state, the probe molecule is less polar compared to the excited state. It is also noticed from Table 2 that there is a considerable increase in Stoke's shift ($\bar{\upsilon}_a - \bar{\upsilon}_f$) with increasing solvent polarity from 2291 to 1645 cm^{-1}, which indicates that there is an increase in the dipole moment in the excited state compared to the ground state.

The dielectric constants, refractive indices, and $\left(E_T^N\right)$ values along with calculated values of various polarity functions are presented in Table 3.

The plots, Stoke's shift vs. $F(\varepsilon,n)$, Stoke's shift vs. $F_1(\varepsilon,n)$, arithmetic mean of Stoke's shift vs. $F_2(\varepsilon,n)$, $\bar{\upsilon}_a$ vs. $F_3(\varepsilon)$, and Stoke's shift vs. E_T^N are presented in Figs. 4, 5, 6, 7, and 8 respectively.

The statistical data like slopes, intercepts, and correlation coefficients are reported in Table 4. It is observed that the correlation coefficient values are around 0.8–0.9, which indicates a good linearity for the respective plots.

From the solvatochromic method using the slopes S_1 and S_2, the value of μ_g from Eq. (16), the value of μ_e from Eq. (17), and their ratio μ_e/μ_g from Eq. (18) are calculated and are given in Tables 5, 6, and 7 respectively. Further, by substituting the value of μ_g determined experimentally from Guggenheim's method in Eqs. (12) to (15), the excited-state dipole moments (μ_e) according to Lippert's, Bakhshiev's, Kawski-Chamma-Viallet's, and McRae's methods are calculated and are given in Table 6. Using the slope calculated from Stoke's shift vs. solvent polarity parameter $\left(E_T^N\right)$, the excited-state dipole moment and change in dipole moment are calculated using Eqs. (22) and (21) respectively and the results are tabulated in Tables 6 and 7.

It is observed from Table 5 that there is a good agreement between μ_g values determined from Guggenheim's and solvatochromic methods. As is evident from Table 6, the μ_e determined by using Bakhshiev's, Kawski-Chamma-Viallet's, and solvatochromic methods are found to be in good agreement with each other. The μ_e calculated using solvent polarity parameter $\left(E_T^N\right)$ is found to be smaller than the excited-state dipole moment determined using Bakhshiev's, Kawski-Chamma-Viallet's, and solvatochromic methods. This may be due to the reason that these methods do not take into account specific solute-solvent interactions like hydrogen bonding, complex formation, and molecular aspects of solvation, whereas they are incorporated in the solvent polarity parameter $\left(E_T^N\right)$ method [27]. The excited-state dipole moment (μ_e) determined from Lippert's and McRae's methods is found to be higher compared to the other methods and it may be attributed to non-accountability of polarizability in these methods [5]. From Tables 5 and 6, it is noticed that the excited-state dipole moments (μ_e) determined from all the methods are found to be higher than the experimental ground-state dipole moment (μ_g) determined from Guggenheim's and solvatochromic methods. The higher values of μ_e indicate that the probe molecule C-334 is more polar or stable in the excited state than the ground state. Further, it is also observed from Table 7 that the $\Delta\mu$ values determined from solvatochromic and $\left(E_T^N\right)$ methods are higher. The higher values of μ_e and $\Delta\mu$ suggest that the probe molecule is more polar or stable in the excited state than the ground state and indicate the existence of more relaxed excited state [41, 42].

Table 6 Excited-state dipole moments by solvatochromic correlations

Excited-state dipole moment (μ_e) (D) from					
Lippert's equation Eq. (12)	Bakhshiev's equation Eq. (13)	Kawski-Chamma-Viallet's equation Eq. (14)	Solvatochromic method Eq. (17)	Solvent polarity parameter Eq. (22)	McRae's equation Eq. (15)
4.614	3.205	3.550	3.757	2.342	4.681

Table 7 Change in dipole moment, ratio, and angle between ground and excited-state dipole moments

Molecule	Change in dipole moment ($\Delta\mu$) (D) from		Ratio of excited- and ground-state dipole moment μ_e/μ_g Eq. (18)	Angle between μ_g and μ_e θ in degree Eq. (19)
	Solvatochromic method Eqs. (16)–(17)	Solvent polarity parameter Eq. (21)		
C-334	2.115	1.252	2.288	0

From Table 7, the angle between μ_g and μ_e is found to be zero. This suggests that the μ_g and μ_e are parallel to each other and the symmetry of the molecule remains unchanged upon electronic transition [39].

4.2 Computational Analysis

The absorption and emission spectra of the probe C-334 for all the studied solvents were computed by using Gaussian 09W in order to compare the maxima values with the experimental results. For this purpose, the probe molecule is optimized for the ground and excited state using DFT and TD-DFT with the basis sets B3LYP/6-31G (d) combined with conductor-like polarizable continuum model (CPCM) solvation model. Further, by using the theoretically computed absorption and emission maxima values, the electronic transition energy for absorption as well as emission were calculated and are tabulated in Table 8. The electronic transition energy values were also determined for the experimental absorption and emission maxima of the probe molecule and are given in Table 8.

From Table 8, it is observed that the experimental and theoretical electronic transition energies for both absorption and emission are found to be in good agreement with each other. In case of absorption, the difference in the experimental and theoretical transition energy is of the order of 0.32 to 0.37 eV, where as in case of emission, it is of the order of 0.27 to 0.39 eV respectively. The experimental transition energies undergo a blue shift in case of absorption as well as emission. Further, it is interesting to note that the theoretical transition energies computed using TD-DFT/CPCM solvation model and the experimental energy values exhibit the similar trend. From Table 2, it is observed that as the polarity of the solvent increases, Stoke's shift increases. From Table 8, it is also observed that as the polarity of the solvent increases, theoretically computed transition energy difference between absorption and emission also increases. From these results, it is noticed that the TD-DFT/CPCM solvation studies reproduce the similar trend as observed experimentally.

The ground-state dipole moment of the probe molecule in the gaseous state is also estimated theoretically by using DFT with basis sets B3LYP/6-31G (d) and the result is presented in Table 5. The optimized molecular geometry of C-334 molecule along with the direction of dipole moment is shown in Fig. 9.

It is observed from Tables 5 and 6 that the theoretically computed μ_g value is higher than the experimental μ_g value. It is to be noted that the experimental methods take solvent and environmental effects like solute-solvent interactions into account, whereas the ab initio computations are based on gaseous phase [27, 43].

Further, in order to analyze the solute-solvent interactions, the ground- and excited-state dipole moments were also estimated theoretically for all the studied solvents by using CPCM solvation model and the results are given in Table 9.

From Table 9, it is noticed that the ground-state dipole moment values for each of the solvents are found to be higher than the ground-state dipole moment value of the probe molecule in the gaseous phase (Table 5). The increase in the dipole moment value is due to the consideration of environmental effects like solute-solvent interactions in the CPCM solvation

Table 8 Experimental and theoretical electronic transition energies of C-334

Solvent	Absorption		Emission	
	E_{expt} (eV)	E_{theory} (eV)	E_{expt} (eV)	E_{theory} (eV)
Benzene	2.793	3.150	2.589	2.980
Tetrahydrofuran	2.793	3.113	2.562	2.835
Propane-2-ol	2.737	3.100	2.500	2.787
Acetone	2.762	3.106	2.500	2.787
Ethanol	2.749	3.104	2.475	2.782
Methanol	2.737	3.109	2.455	2.775
Acetonitrile	2.774	3.105	2.490	2.785

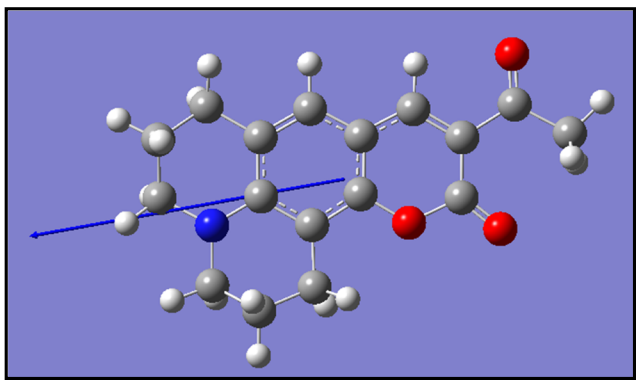

Fig. 9 Ground-state optimized molecular geometry of C-334. The arrow mark indicates the direction of dipole moment

Table 9 Dipole moments of C-334 in different solvents computed using CPCM model

Solvent	Ground-state dipole moment (μ_g) (D)	Excited-state dipole moment (μ_e) (D)
Benzene	10.451	12.733
Tetrahydrofuran	12.056	14.299
Propane-2-ol	12.658	14.832
Acetone	12.657	14.831
Ethanol	12.702	14.879
Methanol	12.752	14.931
Acetonitrile	12.766	14.784

gap. The lower values of energy gap for the probe molecule also support the observed higher values of excited-state dipole moments.

The determination of HOMO-LUMO energies also helps in understanding the chemical stability of a molecule in terms of a parameter known as chemical hardness (η). The molecules possessing large HOMO-LUMO energy gap are considered as hard, whereas molecules possessing small HOMO-LUMO energy gaps are considered as soft molecules [41, 42]. The chemical hardness (η) of a molecule [44] is determined from Eq. (23).

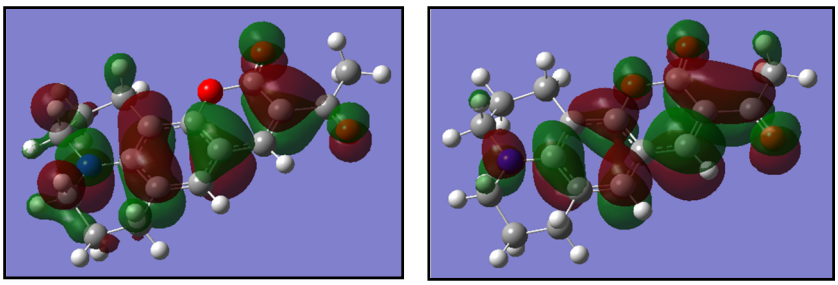

HOMO LUMO

Fig. 10 HOMO-LUMO 3D plots of C-334

model. Further, the excited-state dipole moment values were found to be higher than the corresponding ground-state dipole moment values for all the solvents and this suggests that the probe molecule is more polar in the excited state than the ground state. It is interesting to note that the computational studies also reproduce the similar trend as observed experimentally. However, the theoretically computed ground- and excited-state dipole moments were found to be higher than the experimental dipole moments.

The 3D plots of HOMO and LUMO of C-334 molecule are shown in Fig. 10.

The HOMO, LUMO energies and HOMO-LUMO energy band gap (ΔE) value for the probe molecule are presented in Table 10. The optical band gap E_g^{opt} is determined from absorption threshold wavelength and the result is also tabulated in Table 10. It is observed that the HOMO-LUMO energy band gap is in order with the experimental optical energy band

$$\eta = \frac{[E_L - E_H]}{2} \tag{23}$$

where E_H and E_L are the HOMO and LUMO energies.

The chemical hardness (η) estimated for the probe molecule is given in Table 10. The small values of chemical hardness (η) and HOMO-LUMO energy gaps suggest that the molecule may be considered as soft molecule [41]. These results also support the observed higher values of μ_e.

The molecular electrostatic potential (MESP) plots provide the information for determining a suitable position for nucleophilic and electrophilic attack along with the hydrogen bonding interactions of solvent. The MESP 3D plot of the probe molecule C-334 is shown in Fig. 11. In this plot, different colors correspond to different values of electrostatic potential at the surface. The red color represents negative phase, which can be related to the electrophilic site, and blue color

Table 10 Chemical hardness (η) and energy band gap values of C-334

Molecule	From DFT computations			From absorption spectrum	Chemical hardness (η)
	HOMO (eV)	LUMO (eV)	ΔE[a] (eV)	$\left(E_g^{opt}\right)$[b] (eV)	
C-334	− 5.441	− 1.917	3.524	2.649	1.762

[a] HOMO-LUMO energy band gap obtained using DFT-B3LYP/6-31G (d), ΔE = HOMO-LUMO (eV)

[b] Optical energy band gap calculated from the equation $E_g^{opt} = (hc/\lambda) = 1240/\lambda$ (eV), where λ is the edge wavelength in nm of the UV-Vis absorption spectrum (468 nm in benzene for C-334)

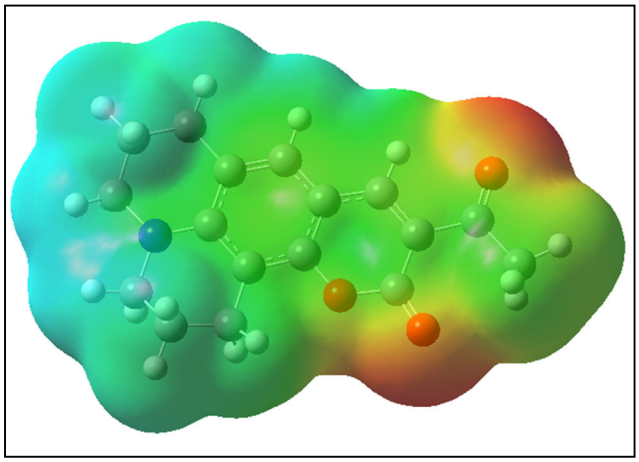

Fig. 11 Molecular electrostatic potential (MESP) 3D plot of C-334

represents positive phase, which corresponds to nucleophilic site. From Fig. 11, it is observed that the MESP plot of probe molecule shows negative phases around 5,6-dihydropyran-2-one and propan-2-one, whereas positive phases around all hydrogen atoms.

5 Conclusions

In the present study, in order to investigate the solvatochromic behavior and dipole moments, the absorption and fluorescence spectra of C-334 were recorded in different solvents. The μ_g value of the probe molecule is determined using Guggenheim's and solvatochromic methods. It is observed that the μ_g determined from these methods are found to be in agreement with each other. The excited-state dipole moments (μ_e) are determined by using Lippert's, Bakhshiev's, Kawski-Chamma-Viallet's, solvatochromic, solvent polarity parameter, and McRae's equations. The μ_e values determined from Bakhshiev's, Kawski-Chamma-Viallet's, and solvatochromic methods are found to be in good agreement with each other. Further, μ_e values determined from different solvatochromic correlations like Lippert's, Bakhshiev's, Kawski-Chamma-Viallet's, McRae's, and solvent polarity parameter are found to be higher than the experimental ground-state dipole moments for the probe molecule under investigation. The changes in dipole moment values ($\Delta\mu$) were found to be higher. This suggests that the probe molecule C-334 is more polar or stable in the excited state than in the ground state and indicates the existence of more relaxed excited state. It is observed that the angle between μ_g and μ_e is found to be zero degree, which suggests that μ_g and μ_e are parallel to each other and there is no change in the symmetry upon electronic transition.

The absorption and fluorescence emission of the probe C-334 were investigated theoretically with the help of Gaussian 09W for all the studied solvents using TD-DFT combined with CPCM solvation model and were compared with the experimental results. It is observed that there is a good agreement between the theoretical and experimental results. Further, the ground- and excited-state dipole moments were also estimated for all the studied solvents by using CPCM solvation model and are compared with the experimental results.

The HOMO-LUMO energy band gaps determined from DFT computations and from optical energy band gap are found to be in order with each other. The chemical hardness (η) investigations suggest that the molecule exhibits the soft nature. The computational studies performed using DFT imply that the probe molecule exhibits both nucleophilic and electrophilic sites.

Acknowledgements The authors are thankful to the authorities of USIC, KUD, for providing the instrumental facility for our research work. One of the authors (CVM) is thankful to the Principal Prof. B.P. Urakadli and staff, Government First Grade College Hubballi, for their continuous support and encouragement.

References

1. N.K. Hamdi, M.M. Chebli, H. Grib, M. Brahimi, A.M.S. Silva, Synthesis DFT/TD-DFT theoretical studies and experimental solvatochromic shift methods on determination of ground and excited state dipole moments of 3-(2-hydroxybenzoyl) coumarins. Journal of Molecular Structure **1175**, 811–820 (2019)
2. N. Khanapurmath, M.V. Kulkarni, L. Pallavi, J. Yenagi, J. Tonannavar, Solvatochromic studies on 4-bromomethyl-7-methyl coumarins. Journal of Molecular Structure **1160**, 50–56 (2018)
3. S. Samundeeswari, M.V. Kulkarni, J. Yenagi, J. Tonannavar, Dual fluorescence and solvatochromic study on 3-acyl coumarins. J. Fluoresc. **27**, 1247–1255 (2017). https://doi.org/10.1007/s10895-017-2052-z
4. J. Basavaraj, H.M. Sureshkumar, S.R. Inamdar, M.N. Wari, Estimation of ground and excited state dipole moment of laser dyes C504T and C521T using solvatochromic shifts of absorption and fluorescence spectra. Spectrochim. Acta Part A-Molecular and Biomolecular Spectro **154**, 177 (2016)
5. U.S. Raikar, V.B. Tangod, S.R. Mannopantar, B.M. Mastiholli, Ground and excited state dipole moments of coumarin 337 laser dye. Optics Communication **283**, 4289–4292 (2010)
6. J. Basavaraj, S.R. Inamdar, H.M. Sureshkumar, Solvent effects on the absorption and fluorescence spectra of 7-diethylamino-3-thienoylcoumarin: Evaluation and correlation between solvatochromism and solvent polarity parameters. Spectrochim. Acta Part A-Molecular and Biomolecular Spectro **137**, 527 (2015)
7. E.J. Schitschek, J.A. Trias, P.R. Hammond, R.A. Henry, R.L. Atkins, New laser dyes with blue-green emission. Optics Communication **16**, 313–316 (1976)
8. C. Parkanyi, M.S. Antonious, J.J. Aaron, M. Buna, A. Tine, L. Cissa, Determination of the first excited singlet state dipole moments of coumarins by the solvatochromic method. Spectro. Letters **27**, 439–449 (1994)
9. E. Perez-Rodriguez, J. Aguilera, F.L. Figueroa, J. Expt, Tissular localization of coumarins in the green alga Dasycladus vermicularis (Scopoli) Krasser: a photoprotective role? Botany **54**, 1093 (2003)
10. K.H. Drexhage, Structure and properties of laser dyes, (Springer-Verlag, Berlin, 1973)

11. J. Thipperudrappa, D.S. Biradar, S.R. Manohara, S.M. Hanagodimath, S.R. Inamadar, R.J. Manekutla, Solvent effects on the absorption and fluorescence spectra of some laser dyes: Estimation of ground and excited-state dipole moments. Spectrochim. Acta Part A- Molecular and Biomolecular Spectro **69**, 991–997 (2008)
12. W.R. Shermon, E. Robins, Fluorescence of substituted 7-hydroxycoumarins. Anal. Chem. **40**, 803–805 (1968)
13. A. Evangelos, P.D. Andrew, Convenient microscale synthesis of a coumarin laser dye analog. Journal of Chemical Education **83**(2), 287 (2006)
14. A. Lacy, R. Kennedy, Studies on coumarins and coumarin-related compounds to determine their therapeutic role in the treatment of cancer. Current Pharmaceutical Design **10**, 3797–3811 (2004)
15. V.U. Jeankumar, R.S. Reshma, R. Janupally, S. Saxena, J.P. Sridevi, B. Medapi, P. Kulkarni, P. Yogeeswari, D. Sriram, Enabling the (3 + 2) cycloaddition reaction in assembling newer anti-tubercular lead acting through the inhibition of the gyrase ATPase domain: lead optimization and structure activity profiling. Organic & Biomolecular Chemistry **13**, 2423–2431 (2015)
16. D. Yu, M. Suzuki, L. Xie, S.L. Morris-Natschke, K.H. Lee, Recent progress in the development of coumarin derivatives as potent anti-HIV agents. Med. Res. Rev. **23**, 322–345 (2003)
17. R.D. Thornes, D.W. Edlow, S. Wood, Inhibition of locomotion of cancer cells in vivo by anticoagulant therapy. I. Effects of sodium warfarin on V2 cancer cells, granulocytes, lymphocytes and macrophages in rabbits. The Johns Hopkins Medical Journal **123**, 305 (1968)
18. D.Z. N'u˜nez, P. Barrias, G.C. Jir'on, M.S.U. Za˜nartu, C.L. Alarc'on, F.E.M. Vieyra, C.D. Borsarelli, E.I. Alarcon, A. Asp'ee, A typical antioxidant activity of non-phenolic amino-coumarins. RSC Advances **8**, 1927 (2018)
19. M. Vaculovicova, S. Dostalova, V. Milosavljevic, P. Kopel, V. Adam, R. Kizek, Characterization of carbon quantum dots by capillary electrophoresis with laser-induced fluorescence detections. J. Metallomics & Nanotechno. **3**, 97 (2015)
20. R. Konecna, H. Viet Nguyen, M. Stanisavljevic, I. Blazkova, S. Krizkova, M. Vaculovicova, M. Stiborova, T. Eckschlager, O. Zitka, V. Adam, R. Kizek, Doxorubicin encapsulation investigated by capillary electrophoresis with laser-induced fluorescence detection. Chromatographia **77**, 1469–1476 (2014)
21. M.H. Kim, H.H. Jang, S. Yi, S.K. Chang, M.S. Han, Coumarin-derivative-based off–on catalytic chemodosimeter for Cu2+ ions. Chemical Communications **4838** (2009)
22. J. Huang, V. Bekiari, P. Lianos, S. Couris, Study of poly(methyl methacrylate) thin films doped with laser dyes. J. Luminescence **81**, 285–291 (1999)
23. C. Reichardt, *Solvents and Solvent Effects in Organic Chemistry*, 3rd edn. (Wiley-VCH, New York, 2004)
24. U.P. Raghavendra, M. Basanagouda, R.M. Melavanki, R.H. Fattepur, J. Thipperudrappa, Solvatochromic studies of biologically active iodinated 4-aryloxymethyl coumarins and estimation of dipole moments. J. Mol. Liq. **202**, 9–16 (2015)
25. S.S. Patil, G.V. Muddapur, N.R. Patil, R.M. Melavanki, R.A. Kusanur, Fluorescence characteristics of aryl boronic acid derivative (PBA). Spectrochim. Acta Part A- Molecular and Biomolecular Spectro **138**, 85–91 (2015)
26. S.K. Patil, M.N. Wari, P.C. Yohannan, S.R. Inamdar, Determination of ground and excited state dipole moments of dipolar laser dyes by solvatochromic shift method. Spectrochim. Acta Part A- Molecular and Biomolecular Spectro **123**, 117–126 (2014)
27. G.V. Muddapur, N.R. Patil, S.S. Patil, R.M. Melavanki, R.A. Kusanur, Estimation of ground and excited state dipole moments of aryl boronic acid derivative by solvatochromic shift method. J. Fluoresc. **24**, 1651–1659 (2014)
28. J.S. Kadadevarmath, G.H. Malimath, N.R. Patil, H.S. Geetanjali, R.M. Melavanki, Solvent effect on the dipole moments and photo physical behaviour of 2,5-di-(5-tert-butyl-2-benzoxazolyl) thiophene dye. Canadian Journal of Physiology and Pharmacology **91**, 1107–1113 (2013)
29. J.R. Manekutla, B.G. Mulimani, S.R. Inamdar, Solvent effect on absorption and fluorescence spectra of coumarin laser dyes: Evaluation of ground and excited state dipole moments. Spectrochim. Acta Part A- Molecular and Biomolecular Spectro **69**, 419 (2008)
30. D.S. Biradar, B. Siddlingeshwar, S.M. Hanagodimath, Estimation of ground and excited state dipole moments of some laser dyes. J. Mol. Struct. **875**, 108–112 (2008)
31. J. Czekella, Two electro optical methods for determination of dipole moments of excited molecules. Chimia **15**, 26 (1961)
32. J. Czekella, Elektrische Fluoreszenzpolarisation: Die Bestimmung von Dipolmomenten angeregter Moleküle aus dem Polarisationsgrad der Fluoreszenz in starken elektrischen Feldern. Z. Elaktrochem. 64, 1221 (1960)
33. M.P. Hass, J.M. Warman, Photon-induced molecular charge separation studied by nanosecond time-resolved microwave conductivity. Chemistry and Physics of Lipids **73**, 35–53 (1982)
34. J.R. Lombardi, Correlation between structure and dipole moments in the excited states of substituted benzenes. Journal of the American Chemical Society **92**, 1831–1833 (1970)
35. E.A. Guggenheim, The computation of electric dipole moments. Transactions of the Faraday Society **47**, 573 (1951)
36. L. Naik, N. Deshapande, I.A.M. Khazi, G.H. Malimath, Resonance energy transfer studies from derivatives of thiophene substituted 1, 3,4-oxadiazoles to coumarin-334 dye in liquid and dye-doped polymer media. Brazilian Journal of Physics **48**, 16–24 (2017). https://doi.org/10.1007/s13538-017-0540-x
37. E.Z. Lippert, Spektroskopische Bestimmung des Dipolmomentes aromatischer Verbindungen im ersten angeregten Singulettzustand. Zeitschrift für Elektrochemie **61**, 962 (1957)
38. N.G. Bakhshiev, Universal intermolecular interactions and their effect on the position of the electronic spectra of molecules in 2-component solutions. Optika i Spektroskopiya **16**(5), 821 (1964)
39. A. Kawski, On the estimation of excited state dipole moments from solvatochromic shifts of absorption and fluorescence spectra. Zeitschrift für Naturforschung **57A**, 255 (2002)
40. U.S. Raikar, V.B. Tangod, B.M. Mastiholli, S. Sreenivasa, Solvent effects and photophysical studies of ADS560EI laser dye. African Journal of Pure and Applied Chemistry **4**(9), 188 (2010)
41. K.B. Akshaya, V. Anitha, L.L. Prajwal, K. Rekakumari, G. Louis, Synthesis and photophysical properties of a novel phthalimide derivative using solvatochromic shift method for the estimation of ground and singlet excited state dipole moments. Journal of Molecular Liquids **224**, 247–254 (2016)
42. A. Roshmy, V. Anita, G. Louis, N. Aatika, Estimation of ground state and excited state dipole moments of a novel Schiff base derivative containing 1,2,4-triazole nucleus by solvatochromic method. J. Mol. Liq. **215**, 387 (2016)
43. S.R. Manohara, V.U. Kumar, G.L. Shivakumaraiah, Estimation of ground and excited-state dipole moments of 1, 2-diazines by solvatochromic method and quantum-chemical calculation. J. Mol. Liq. **181**, 97–104 (2013)
44. R.G. Pearson, *Chemical Hardness* (Wiley - VCH, Weinheim, 1997)